ORIGINAL ARTICLE

Total knee arthroplasty three-dimensional kinematic estimation prevision. From a two-dimensional fluoroscopy acquired dynamic model

B.P. Lebel[a,*], V. Pineau[a], S.L. Gouzy[a], L. Geais[b], J.-J.M. Parienti[c], J.-J.P. Dutheil[c], C.H. Vielpeau[a]

[a] Orthopedic Department, Caen University Hospital, avenue de la Côte-de-Nacre, 14033 Caen cedex, France
[b] Reasearch and Development, Stryker SA, Europe
[c] Biostatistic Department, Caen University Hospital, Caen, France

Summary
Introduction: To determine six-degree of freedom of total knee arthroplasty kinematics (TKA), optimized matching algorithms for single fluoroscopic image system may be used. Theoretical accuracy of these systems was reported. Nevertheless, all reports were done under idealized laboratory experimental conditions. The aim of this study was to evaluate the ''true'' accuracy of a flat panel single plane video-fluoroscopy system based on computed-assisted design (CAD) model matching and compare it to TKA kinematics obtained from optoelectronic measurements as gold standard.
Hypothesis: The estimation of the error produced by 2D/3D fluoroscopic registration in daily practice is misjudged in most available laboratory reports.
Material and methods: The experimental set-up used a TKA implanted into femoral and tibial cadaver bones. Thirty flexions were simultaneously registered using single plane fluoroscopy and an active optical tracking system. Kinematics registered were compared using the root mean square error (RMS), the concordance correlation coefficient and Bland & Altman plot analysis.
Results: The mean range of motion of flexion during the experiment was 106°. The respective RMS for flexion, varus-valgus and internal-external rotation were 0.68, 0.67 and 1.02°. The respective RMS for antero-posterior, medio-lateral and proximo-distal displacement were 1.3, 2.4 and 1.06 mm. Extreme values of the measured error concerning medio-lateral displacement were −5.4 and 22,1 mm.

* Corresponding author. Tel.: +33 2 31 06 48 09; fax: +33 23 10 64 85 09.
E-mail address: Lebel-b@chu-caen.fr (B.P. Lebel).

Discussions: Analysis found some outliners in all degree of freedom with a systematic error and larger standard deviation than already published data. One should make sure that during the experiment the motion of interest is in the in-plane direction. Moreover, this study brings out the true threshold detection of this type of analysis.
Level of evidence: Level 3. Prospective diagnostic study.

Introduction

Accurate in vivo kinematics analysis of total knee arthroplasty (TKA) is primordial to understand the knee joint mechanics after surgery. Better understanding of knee joint mechanics could lead to improved implant design, better surgical strategies, and increased longevity of the implant components. The importance of studying active knee kinematics for future enhancement in the treatment of the arthritic knee was well illustrated in the literature [1]. Several methods to investigate in vivo TKA kinematics have been proposed. Peroperative optoelectronic measurement is one of them. The two major problems with this approach are the fact that the data provided concern only passive motion and the invasive character of this method. Nevertheless, it is a highly accurate and recognized tool to measure in vivo knee passive kinematics. Electromagnetic-goniometers are useful for direct movement measurements [2]. Crosstalk due to rotation between the endblocks is however a well-known inaccuracy problem. Instrumented gait analysis is also a well-established method for gathering in vivo kinematics and kinetics data of knee joint. The main problem with this approach is the error caused by skin movement artifacts [3,4]. Dual plane video-fluoroscopy is another method [5–7]. Nevertheless, this procedure requires specific equipment non available in all hospital. That is why single plane video-fluoroscopy gets an important place in this field. In this method, a registration algorithm estimates the pose of the implant components from the single plane projection view of the fluoroscopic image series.

Since 1996, different 2D/3D registrations techniques have been proposed. Theoretical accuracy and optimization methods have also been investigated [8]. However, there is a common lack of accuracy of all these methods, especially in the out of plane translation estimation. Moreover, most accuracy reports were done using a static model under controlled idealized conditions and standardized geometric shapes. To our knowledge, no previous study has presented simultaneous kinematics from either 2D/3D registration technique and computer-assisted measurement in a dynamic model reproducing assessment conditions of the ''real life''. The goal of this study was to evaluate the accuracy of our flat panel single plane video-fluoroscopy system based on computed-assisted design (CAD) model matching, using TKA kinematics obtained from optoelectronic measurement as gold standard. Our hypothesis was that the estimation of the error produced by 2D/3D fluoroscopic registration in daily practice is misestimated by available laboratory reports. Reporting the ''true'' accuracy of this system under real conditions will allow us to better analyze further clinical findings.

Material and methods

The TKA model and experimental setting was as follows. Femoral and tibial components of the Triathlon® total knee prosthesis (Stryker, Mahwah, NJ) were used. A postero-stabilized (PS) femoral implant (size 4) and a tibial component (size 4) with a PS polyethylene insert (8 mm of thickness) were fixed to cadaver bones using polymethylmethacrylate resin. The 3D Euclidean orientation of the CAD model was set as presented in the Fig. 1. Medial and lateral ligament were modelized using elastic band. They were fixed onto the bone using metal screws. Active Trackers for optoelectronic analysis were fixed onto the bones segments using anchoring pins. Then, this TKA model was manually moved from extension to flexion (mean flexion archived was $106 \pm 16°$). The tibia was maintained fixed into one of the examiner hand and the femur was flexed with the other hand. This was done to simulate flexion task (stair climbing, weight-bearing flexion) usually achieved in clinical experiment [9,10]. Kinematics were simultaneously assessed using 2D fluoroscopic images and optoelectronic system. We registered 30 non-consecutives flexions using this two measurement systems. Fig. 2 presents the experimental setting.

The model-based fluoroscopic kinematics were assessed as follows. Fluoroscopic images were acquired using a Phillips flat panel system. We registered 30 images per sec-
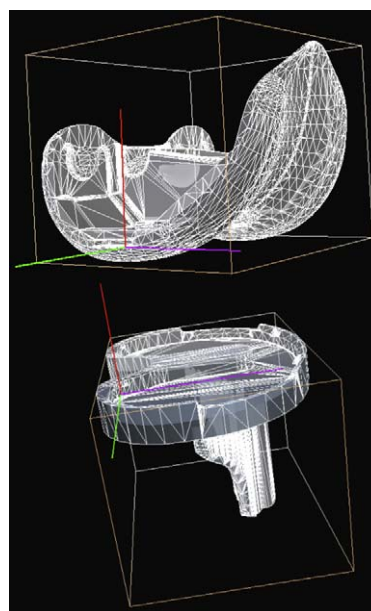

Figure 1 The 3D Euclidean orientation of the Triathlon® components CAD models. Femoral (OF, xF, yF, zF) and tibial (OT, xT, yT, zT) implants coordinate system are shown. (x = red line, y = green line, z = purple line).
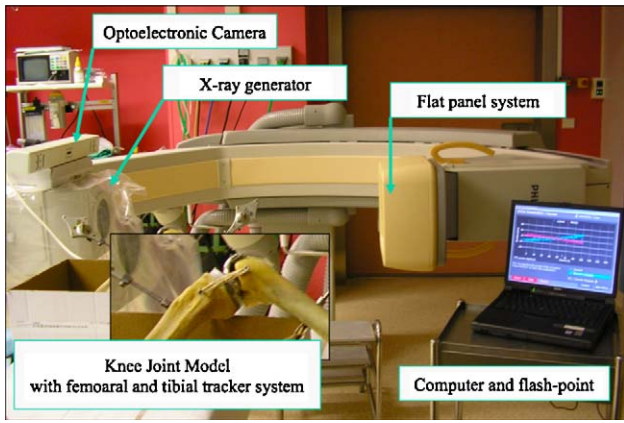
Figure 2 Experimental setting showing the TKA model with the anchoring pin and the fluoroscopic field associated to the optoelectronic set-up.

ond. The image resolution was 75 dpi. Then, all images were treated using model-based analysis software (MBRSA v3.2, Medis, The Netherlands) validated by Garling [11]. The technique is based on minimizing the difference between the virtual projection of a 3D surface model of an implant with the actual projection of the implant as it appears in a roentgen image. The actual contour of the implant in the radiograph was detected by means of the Canny algorithm [12]. Note that the contour can consist of multiple contour parts that do not necessarily form a closed contour. By means of computer graphic techniques, the 3D model of the implant was projected onto the image plane and a virtually projected contour was calculated [13]. The actual contour and the virtual contour were defined as a chain of nodes. The difference between the actual contour and the virtual contour is defined as the mean distance between the nodes of the actual contour and the virtual contour. In order to calculate the three-dimensional position and orientation
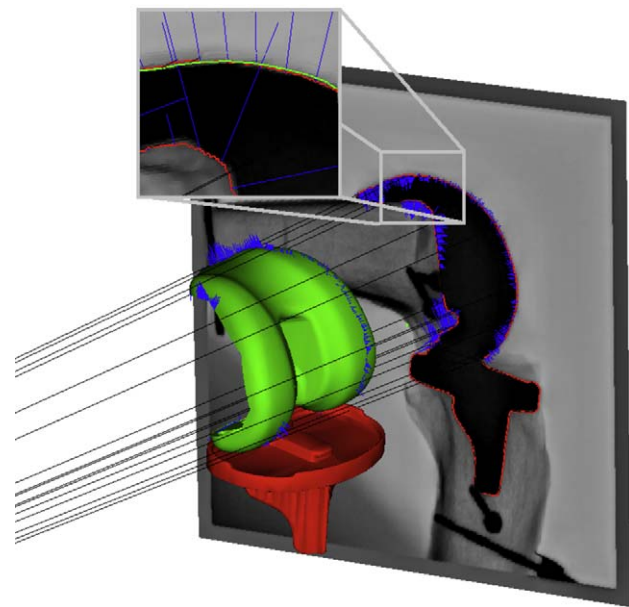

Figure 3 Detail of the fluoroscopic view with the detected contour (green line) and the match projected contour (red line). The perpendicular line (blue) is the 10 times enlargement of the shortest line connecting the actual and virtual contour.

of the implant, the contour difference between the actual contour and the virtual contour was minimized. To accomplish this, first the pose of the implant was set by a human operator. Secondly, an iterative inverse perspective matching (IIPM) algorithm was used. This algorithm is based on the work of Wunsch and the iterative closest point (ICP) algorithm of Besl [14,15]. Then, to finalize the projected contour optimization, we used an optimization algorithm as presented by Valstar [13]. Fig. 3 illustrates a detail of the actual contour and the matched virtual contour. This procedure was done either for the femoral component and the
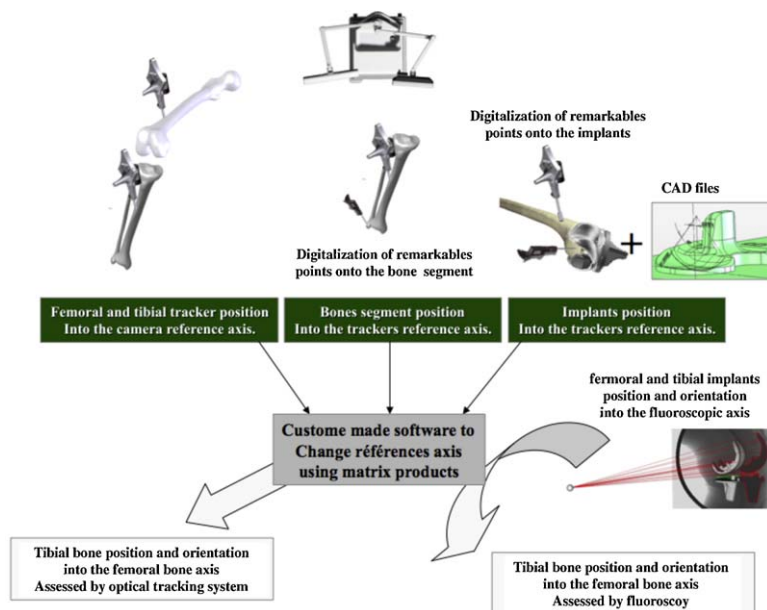

Figure 4 Chart illustrating the methods to compare both kinematics assessment techniques.

tibial component. From this analysis, the position and pose of both CAD models into the fluoroscopic axis system were obtained.

Computer-assisted kinematics were assessed as follows. An active optical tracking system (IGT-Leibinger-Stryker) was used. It was composed of IGT cameras 580 mm (3 LED 50 mm active IGT), a flashpoint (i5000, IGT-Leibinger-Stryker) and two active trackers. Femoral tracker was anchor into the anterior femoral diaphysis bone. Tibial tracker was anchor into the anterior tibial diaphysis bone. We registered the femoral and the tibial tracker position and orientation into the IGT camera coordinate axis with the corresponding timestamp. In order to match data assessed with optical system to data assessed with single plane fluoroscopy, remarkable points were digitalized onto femoral and tibial bone using an active probe to orientate bones segments into the camera coordinate axis system (hip center, distal femur center, proximal tibia center, ankle center, medial and lateral epicondyles). Then, remarkable points were digitalized onto femoral and tibial implants to orientate implants into the camera coordinate axis system (lateral and medial edge of the tibial implant, upper surfaces of the tibial implant, medial and lateral inner surfaces of the femoral component, medial and lateral femoral implants' condyles). Up to 500 points were digitalized onto both components.

Then, to compare both kinematics assessments, concordance of the fluoroscopic and computed axis system was made. We had arbitrarily chosen to compare tibial bone kinematics into the femoral bone coordinate system of both measurement systems. However, data provided by both measurement techniques had a different reference frame. Indeed, using optoelectronic assessment, kinematics data concerned bone kinematics. Using 2D/3D registration, kinematics data concern the implants kinematics. Therefore, reference frame of both measurement were matched using matrix transfer of Euler angles and Chales' theorem [16]. Fig. 4 illustrates the references and origins' changes realized to be able to compare kinematics. The following matrix was used to set pose and position of the tibial bone into the femoral bone reference frame.

Figure 5 Origins and reference frame of tibial and femoral bones. The femoral coronal plane is the plain containing the hip center and both epicondyles. The femoral center was set as the mid distance between the epicondyle. Sagittal and transverse plane were the two orthogonal planes to the coronal plane crossing each other at the femoral center. The same construction was made for tibial planes.

interest and stated sign (positive or negative) to describe kinematics. Kinematics was presented as the kinematics of the tibia into the femoral plane. Finally, we obtained knee joint kinematics registered by both techniques associated to the corresponding timestamp.

Results were analyzed and reported using Medcalc® software (version 10.1.8.0). Kinematics data of the model assessed using computed optical system were first presented. They were reported as the evolution of the rotations

$$
MT \rightarrow F = \begin{bmatrix} \cos(\beta) * \cos(\gamma) & -\cos(beta) * \sin(\gamma) & \sin(\beta) & x \\ \sin(\alpha) * \sin(\beta) * \cos(\gamma) + \cos(\alpha) * \sin(\gamma) & -\sin(\alpha) * \sin(\beta) * \sin(\chi) + \cos(\alpha) * \cos(\gamma) & -\sin(\alpha) * \cos(\beta) & y \\ -\cos(\alpha) * \sin(\beta) * \cos(\gamma) + \sin(\alpha) * \sin(\gamma) & \cos(\alpha) * \sin(\beta) * \sin(\gamma) + \sin(\alpha) * \sin(\gamma) & \cos(\alpha) * \cos(\beta) & z \\ 0 & 0 & 0 & 1 \end{bmatrix}
$$

Both analyses provided pose and orientation of the tibia into the femoral reference frame. From those data we obtained the six necessary parameters to describe bone kinematics as follow. First, tibial and femoral bones reference frame were defined as explain in the Fig. 5. Then, we defined the three rotations and the three translation distances using projections of implant vectors on the corresponding referent plane. As example, Flexion angle was defined as the angle between the projection of proximodistal femoral and tibial implant vectors into the femoral sagittal plane of the femoral bone. Translations were obtained similarly in measuring the distance between the projection of tibial bone (OT) and femoral bone (OF) center projection on the referent axis. Table 1 resumed vector of
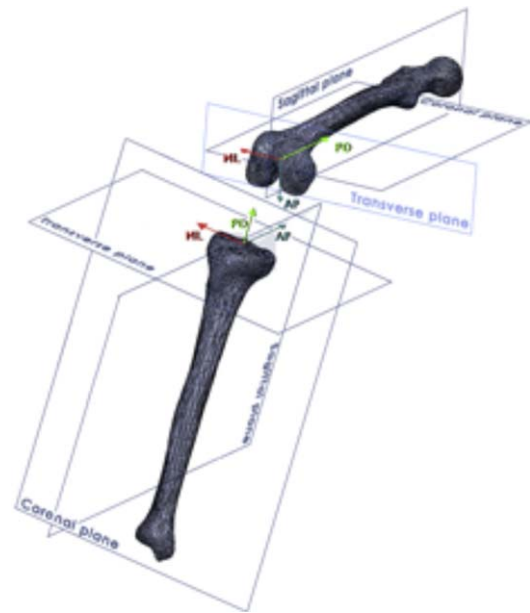
and translations plotted to the flexion path. Kinematics pattern registered using computed optical system during the 30 flexions was reported as a graph of average motion for the flexing paths according to the six degrees of freedom. Data of both assessment tools were match according the timestamp; data with more than 0.01 second of mismatch were excluded. Then, the relative accuracy of 2D/3D registration taking optical computed assessment as gold standard was assessed using the root mean square error (RMS). The concordance correlation coefficient (CCC) [17] was also used to evaluate the degree to which pairs of observations fall on the 45° line through the origin with his 95% confidence interval. The Bland & Altman plot [18] was also used to compare these two measurements techniques.

Table 1 Definitions of kinematics from tibial and femoral planes and vectors of tibial and femoral reference frames.

Degree of freedom	Vectors used or points of interest	Referent plane or axis of projection	Negative value (tibial motion)	Positive value (tibial motion)
Flexion/extension	Tibial and femoral PD	Femoral sagittal plane	Extension	Flexion
Varus/valgus	Tibial and femoral ML	Tibial frontal plane	Valgus	Varus
Internal/external rotation	Tibial and femoral ML	Tibial coronal plane	Internal rotation	External rotation
Antero-posterior displacement	OF and OT	AP tibial axis	Anterior	Posterior
Medio-lateral displacement	OF and OT	Ml tibial axis	Lateral	Medial
Proximo-distal displacement	OF and OT	PD tibial axis	Proximal	Distal

OF: femoral center; OT: tibial center; PD: proximo-distal; ML: medio-lateral.

Table 2 Speed and range of motion achieved with the presented knee model assessed using optoelectronic system. The arithmetic mean was the mean value observed during the 30 flexions. Minimum value, maximum value and standard deviation of each flexion were also presented.

$n = 30$	Arithmetic mean	Minimum value	Maximum value	Standard deviation
Flexion time (second)	1.6	1.1	2.4	0.3
Range of motion of flexion (degree)	106.3	79.6	135.8	16.29
Range of motion of varus/valgus (degree)	−3.5	−0.8	−5.5	1.16
Range of motion of internal/external rotation (degree)	−0.08	−7.3	6.1	4.3
Range of motion of antero-posterior displacement (mm)	−15.4	−10.1	−22.8	3.4
Range of motion of medio-lateral displacement (mm)	−3.2	−7.5	2.9	2.4
Range of motion of proximo-distal displacement (mm)	−14.1	−17.3	−9.5	2.0

In this graphical method the differences between the two techniques are plotted against the averages of the two techniques. This analysis was completed by Mountains plots analysis. A mountain plot (or ''folded empirical cumulative distribution plot'') was created by computing a percentile for each ranked difference between fluoroscopy method and optoelectronic method. These percentiles were then plotted against the differences between the two methods [19].

Results

Resumed data characterizing the 30 non-consecutives joint flexions obtained using optoelectronic assessment are presented in the Table 2. We found during knee flexion motion that varus-valgus and all three components of translation were correlated to flexion angle ($P < 0.001$). This relationship was illustrated concerning varus angle and antero-posterior distance in the Fig. 6. However, rotation
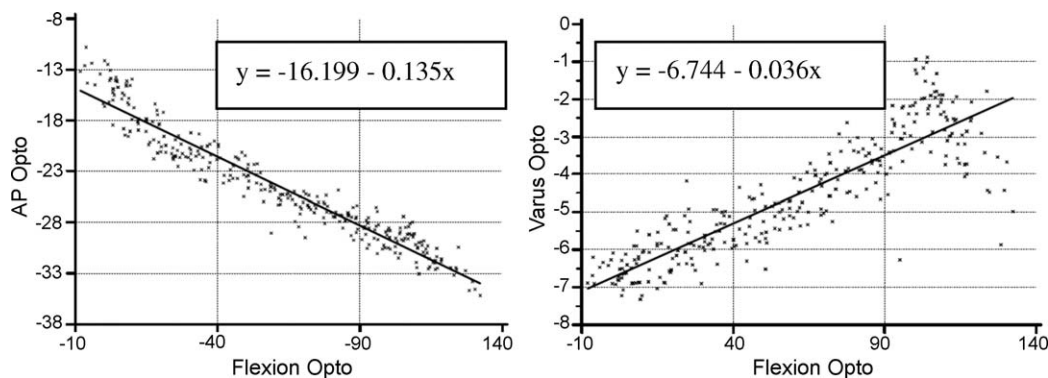

Figure 6 Value of antero-posterior distance and varus/valgus rotation plotted to the flexion angle.

Table 3 Accuracy results of single plane fluoroscopy presenting the RMSE into the 6 degree of freedom.

n = 336	RMS	Mean difference	Standard deviation	Minimum value	Maximum value
Flexion (degree)	0.687	0.054	0.981	−5.63	3.27
Varus (degree)	0.671	0.051	0.856	−4.2	1.8
Internal rotation (degree)	1.026	0.481	1.284	−5.2	3.9
Antero-posterior displacement (mm)	1.310	−0.521	3.331	−6.66	3.22
Medio-lateral displacement (mm)	2.438	0.731	3.942	−5.4	22.1
Proximo-distal displacement (mm)	1.063	0.093	1.364	−4.65	3.64

was independent from the flexion angle (Correlation coefficient: −0.002, 95% CI [−0.131, 0.081]) if we considered the data obtained during the thirty flexions motions. Nevertheless, in each of the thirty flexions motion, a statistical relationship between flexion and internal-external rotation was observed. To be more illustrative, kinematics of the model coupling flexion, antero-posterior displacement and rotation registered using optoelectronic system during the 30th flexion was presented as the projection of the medio-lateral femoral bone line onto the tibial insert (Fig. 7).

In this experiment, accuracy of the 2D/3D registration was defined as the differences with optoelectronic measurement. These techniques were compared in 336 relatives' poses and positions of bone segments. The RMS error between these two assessment tools was less than 1.1 degree for rotation, flexion, and varus, and less than 1.5 mm for the antero-posterior and proximo-distal translations. The RMS and the mean difference were higher for the medio-lateral translation ($P < 0.001$), which was in the fluoroscopic plane. Detailed results are presented in the Table 3. Moreover, mountain plot analysis showed that the medio-lateral translation error had the higher range of value between the 2.5th and the 97.5th percentile (central 95% of the data) ($P = 0.002$) (Fig. 8). The CCC was almost perfect for the flexion angle (CCC = 0.9997) comparing the two assessment methods. Concerning the other rotation, The CCC were respectively of 0.88 for internal/external rotation and 0.89 for varus/valgus angle. Concerning translation, the ICC was also high for antero-posterior and proximo-distal displacement (0.964 and 0.941). However, medio-lateral displacement had shown the lowest CCC with a score at 0.102 (95% CI [0.024−0.186]). Bland and Altman analysis found interesting results (Fig. 9). It pointed out an absolute systematic error in the medio-lateral, proximo-distal, and varus/valgus displacement measurement. Compared to optoelectronic analysis, single plane fluoroscopy underestimate the proximo-distal displacement ($P < 0.001$) for minus value, and over-estimate medio-lateral displacement and varus rotation ($P < 0.001$) for minus value. Outliers were also pointed out, a second analysis of those points found results range into the 1.96 standard deviation.

Discussion

The goal of this study was to evaluate the accuracy of our single plane video-fluoroscopy system based on CAD model matching using TKA kinematics obtained from computer-assisted measurement as gold standard. Contrary to others, this study was intended to investigate accuracy in dynamics conditions using modern flat panel fluoroscopic installation. This report found the minimal accuracy for internal/external rotation and medio-lateral displacement measurements. However, rotations in varus/valgus and flexion/extension and translation in the antero-posterior and proximo-distal displacement were more accurate. Moreover, some large errors have been observed in all degree of freedom. Outliers' data may have different origins. The human intervention in validate contouring is one of them. These large errors can also be caused by a number of reasons, such as increased with range of motion, the transformation matrix used, misalignment of markers (trackers), and matching methods based on the timestamp used in this study.

Kinematics achieved with this simple model were not so far from reality. Model ranges of motions were not completely comparable to kinematics reported after TKA procedure [20]. The thirty flexions realized were not similar regarding the flexing path especially for rotation pattern. However, a relationship between flexion and rotation was found by analyzing each flexion movement separately. This different rotation pattern into the thirty flexions motions may be explained by the manual rotation strength applied by the operator during flexion. Therefore, the thirty movements registered were different from each other simulated thirty different patients.

Different 2D/3D registration techniques have been proposed. The pioneers, Banks and Hodge [21], proposed a method designated as a pattern matching in which the contours of pre-computed 2D images generated using a computer generated precise geometric model of a knee prosthesis in various poses are stored in a library. Then, the position/orientation of the actual prosthesis is based on a matching criterion. Zuffi et al. [22] developed a
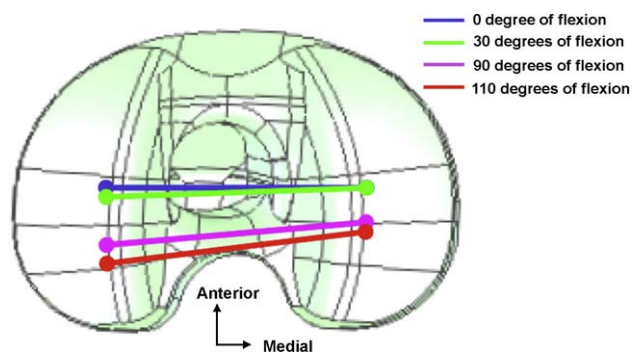

Figure 7 Schematic view of kinematics achieved during the 30th flexion. The medio-lateral femoral line was projected onto the tibial insert at different flexion angle.
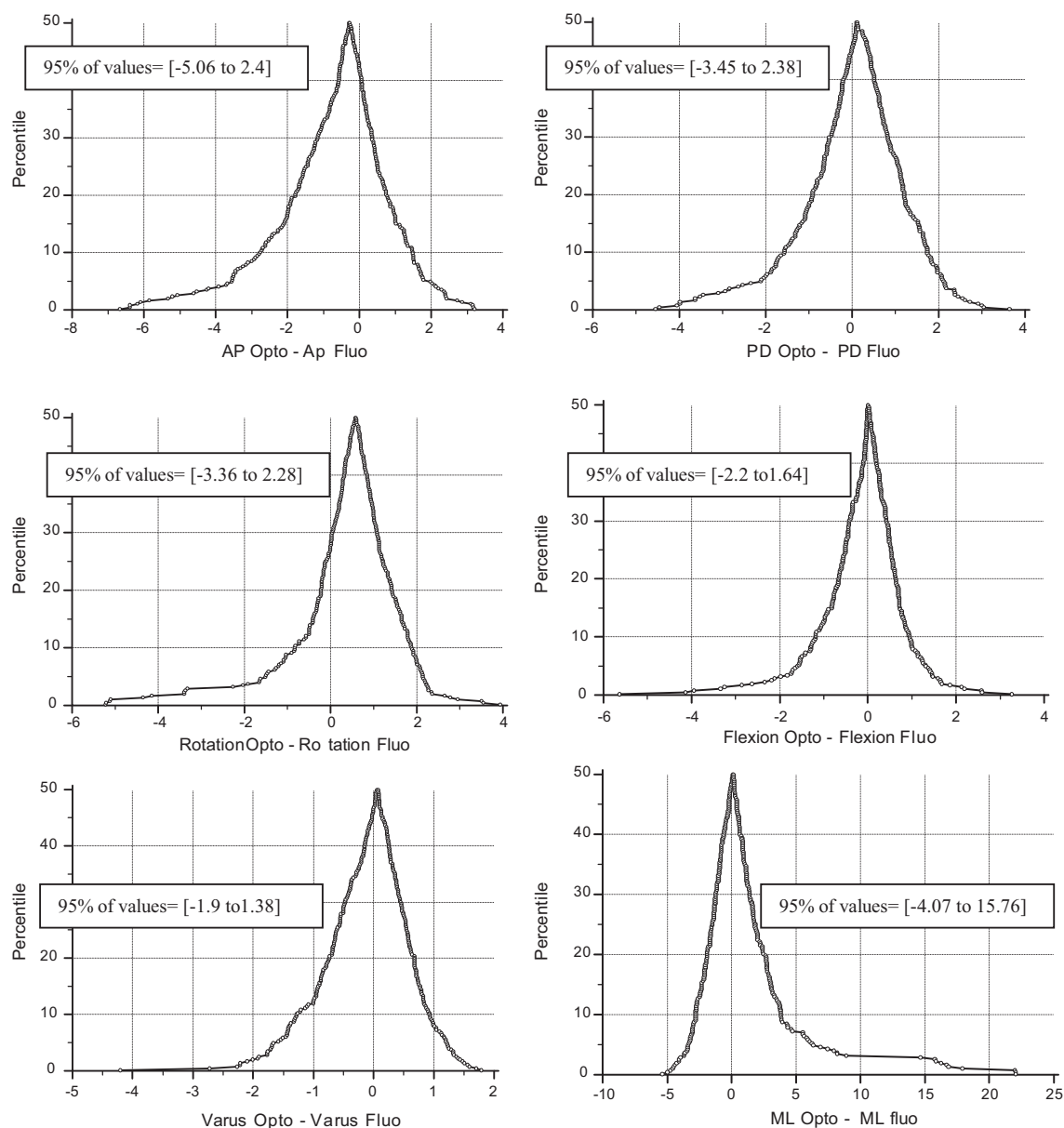
Figure 8 Mountains plots analysis showing the 95% central value for each six-degree of freedom.

method for measuring TKA kinematics, in which matching was performed by rotating/translating the computer model to minimize the Euclidean distance of the model surface from the projection rays drawn from the projection center to the detected contour of the prosthetic X-ray images. Mahfouz et al. [12] measured the similarity between a direct X-ray image and a registered computer model image. Any of the above mentioned methods have merits and demerits. We choose a different approach using the matching process proposed by Kaptein [24] in his model-based RSA proposal and later used by Garling et al. [11] in their analysis of mobile-bearing TKA kinematics. This analysis process had the advantage to allow silhouettes of the two components to overlap. Accuracy of this technique depends on many factors as accuracy of the computerized model, symmetry of the model, and image quality. Fukuoka et al. [25] clearly show that the image quality is an important point. In stan-

dard fluoroscopy set-up, different adaptations are made to overcome the pincushion distortion [26] and to calibrate the system [27]. We used a flat panel detector that recently makes an entrance into this field. This technology allows for availability of distortion free images, high contrast resolution, large dynamic range and high sensitivity to X-ray. In our experiment, an independent method using an optical sensor system was used to test the ground truth. Although ideally the ground truth data should be much more accurate than system being tested, the measurement error contains contribution from both assessment measures. Mafhouz et al. [23] analytically estimated the contribution of the error in the relative pose measurement due to the Optotrack® and showed that it was a significant fraction of the measured error. We used an active system of last generation, which is theoretically more accurate with a static precision of 0.001 mm. Nevertheless, dynamic accuracy of this type of
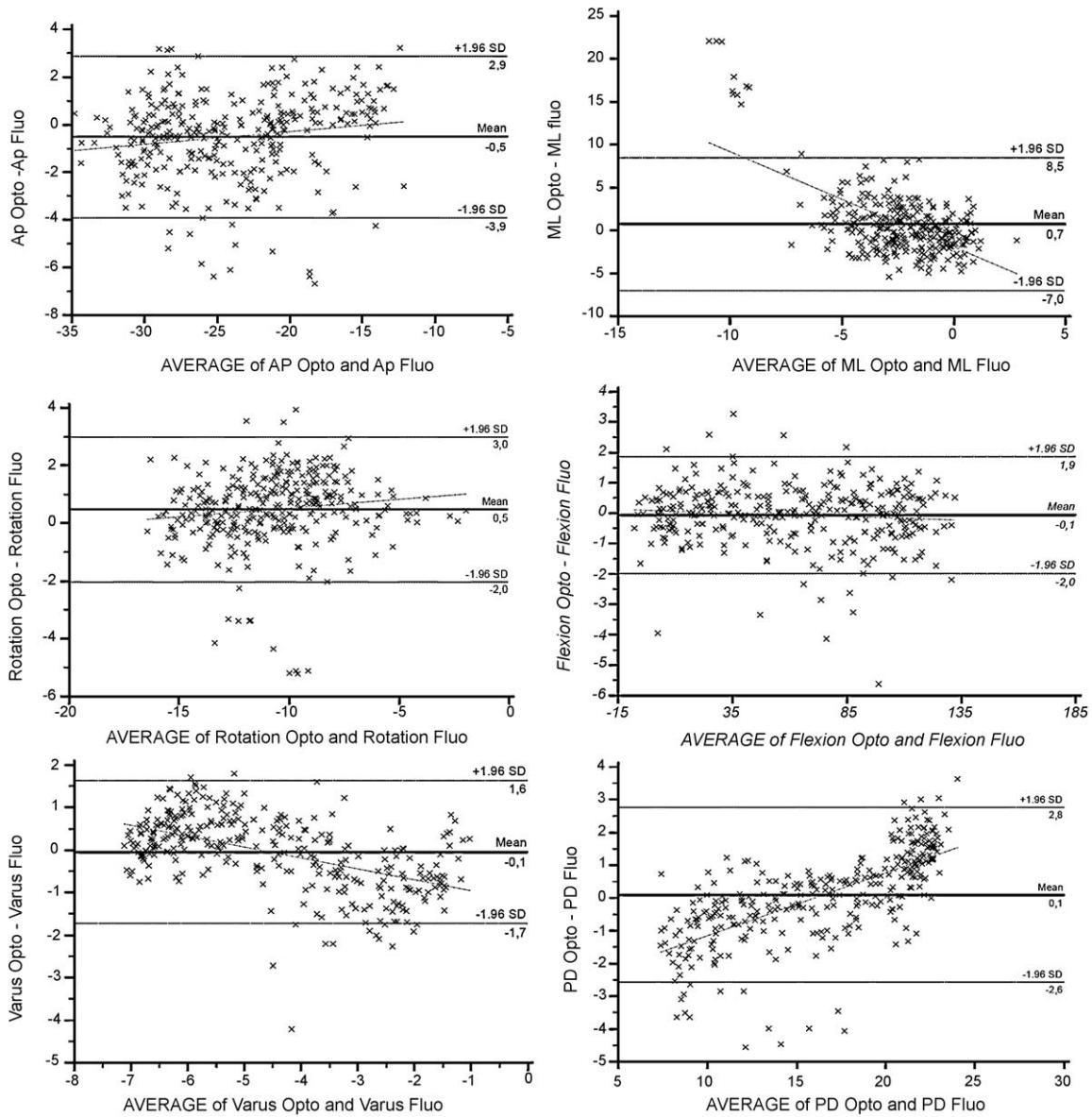
Figure 9   Bland and Altman analysis comparing the two assessment methods into the six-degree of freedom.

system remains underreported in the literature. Therefore, we also assume that a part of the measured error could be due to the optoelectronic system.

Our main hypothesis was confirmed. This study reports higher inaccuracy than those reported by others studying the theoretical accuracy into perfect condition. Most of the time, authors had investigated this parameter using computed simulations. Idealized environments were created in order to determine the matching algorithms repeatability, accuracy, sensitivity to model point density and pose orientation, and optimal parameters under controlled condition. These tests gave a basis for the ultimate potential of the algorithm. However, accuracy estimated under these conditions is not the 'real' accuracy in clinical practice. Zuffi et al. [22] found a different performance of their methods between computer simulation and in vivo test justified by the inaccuracy of contour extraction and by the representation of the imaging process with the perspective projection

model using their techniques. Table 4 compares our accuracy assessment to other reports with different experimental condition and different fluoroscopy analysis process.

Since we reported dynamic kinematics data, we choose to report accuracy in the 6 degree of freedom of the knee joint. Other accuracy and comparative reports had presented data in the fluoroscopy axis system. This also complicates comparisons to already published data. Moreover, not all authors presented their complete results including outliers and the 95% central value. Mafhouz et al. [23] compared pose estimation assessed using 2D/3D registration with pose estimation assessed by an Optotrak system (Nothern digital Inc., Canada). They used knee cadaver in static position. Pose and position of the implant were estimated for each knee position in probing the implant with a probe tip. They found significant differences in function of the fluoroscopic view. Magnitude of Z (out of plane) error passed from 4.7 mm in the frontal view to 1.7 mm in the

Table 4 Comparison to accuracy of single plane fluoroscopy already reported.

Authors	Algorithm type	In-plane accuracy		Out of plane accuracy	
		mm	deg	mm	deg
Banks and Hodge [21]	Template matching	0.20	0.30	2.00	0.3
Zuffi et al. [22]	Hypothesis & test IPP	0.4	0.4	2.0	0.4
Mafhouz e tal. [23]	Hypothesis & test DRR	0.66	1.5	3.21	1.5
Garling et al. [11]	Hypothesis & test IPP	0.17	0.3	1.9	0.3
This study	Hypothesis & test IPP	1.31	1.1	2.4	0.7

sagittal view of the implant. During flexion, orientation of the implant changes into the 6 degree of freedom. This fact partly explains the systematic error founded concerning proximo-distal displacement and varus-valgus rotation. In other words, accuracy of 2D/3D registration changes during the flexion motion. This was well illustrated by Bland and Altman analysis presented in this report. One should take care that during the experiment the motion of interest is in the in-plane direction.

To conclude, despite some large error, the 2D/3D registration technique used in this experiment remain a useful tool to investigate the 3D kinematics of TKA implants using standard equipment, without any fastidious calibration process. Nevertheless, we recommend a double examination of repeated movements assessment to recognize and eliminate some of the outlier's data. Results reported bring out the true threshold detection limit of 2D/3D registration technique.

Disclosure of interest

Acknowledgment

References

[1] Andriacchi TP, Dyrby CO, Johnson TS. The use of functional analysis in evaluating knee kinematics. Clin Orthop Relat Res 2003;410:44—53.

[2] Migaud H, Gougeon F, Diop A, Lavaste F, Duquennoy A. Cinematic in vivo analysis of the knee: a comparative study of 4 types of total knee prostheses. Rev Chir Orthop Reparatrice Appar Mot 1995;81(3):198—210.

[3] Andriacchi TP, Alexander EJ, Toney MK, Dyrby C, Sum J. A point cluster method for in vivo motion analysis: applied to a study of knee kinematics. J Biomech Eng 1998;120(6):743—9.

[4] Stagni R, Fantozzi S, Cappello A. Propagation of anatomical landmark misplacement to knee kinematics: performance of single and double calibration. Gait Posture 2006;24(2):137—41.

[5] You BM, Siy P, Anderst W, Tashman S. In vivo measurement of 3-D skeletal kinematics from sequences of biplane radiographs: application to knee kinematics. IEEE Trans Med Imaging 2001;20(6):514—25.

[6] Li G, Wuerz TH, DeFrate LE. Feasibility of using orthogonal fluoroscopic images to measure in vivo joint kinematics. J Biomech Eng 2004;126(2):314—8.

[7] Bingham J, Li G. An optimized image matching method for determining in vivo TKA kinematics with a dual-orthogonal fluoroscopic imaging system. J Biomech Eng 2006;128(4):588—95.

[8] Hirokawa S, Abrar Hossain M, Kihara Y, Ariyoshi S. A 3D kinematic estimation of knee prosthesis using X-ray projection images: clinical assessment of the improved algorithm for fluoroscopy images. Med Biol Eng Comput 2008;46(12):1253—62.

[9] Asano T, Akagi M, Tanaka K, Tamura J, Nakamura T. In vivo three-dimensional knee kinematics using a biplanar image-matching technique. Clin Orthop Relat Res 2001;388:157—66.

[10] Stiehl JB, Dennis DA, Komistek RD, Keblish PA. In vivo kinematic analysis of a mobile bearing total knee prosthesis. Clin Orthop 1997;345:60—6.

[11] Garling EH, Kaptein BL, Geleijns K, Nelissen RG, Valstar ER. Marker configuration model-based roentgen fluoroscopic analysis. J Biomech 2005;38(4):893—901.

[12] Canny JA. A computational approach to edge detection. IEEE Trans Pattern Anal Mach Intell 1986;8:679—98.

[13] Valstar ER. Digital Roentgen stereophotogrammetry. Development, validation, and clinical application. Thesis, Leiden University, ISBN 90-9014397-1: Pasmans BV, Den Haag; 2001.

[14] Wunsch P, Hirzinger G. Registration of CAD-models to images by iterative inverse perspective matching. Proceedings of the 1996 International Conference on Pattern Recognition. Vienna, Austria; 1996. p. 77—83.

[15] Besl PJ, McKay ND. A method for registration of 3-D shapes. IEEE Trans PAMI 1992;14:239—56.

[16] Spoor CW, Veldpaus FE. Rigid body motion calculated from spatial co-ordinates of markers. J Biomech 1980;13:391—3.

[17] Lin LIK. A concordance correlation coefficient to evaluate reproducibility. Biometrics 1989;45:255—68.

[18] Bland JM, Altman DG. Statistical method for assessing agreement between two methods of clinical measurement. Lancet 1986;i:307—10.

[19] Krouwer JS, Monti KL. A simple, graphical method to evaluate laboratory assays. Eur J Clin Chem Clin Biochem 1995;33:525—7.

[20] Morra EA, Rosca M, Greenwald JF, Greenwald AS. The influence of contemporary knee design on high flexion: a kinematic comparison with the normal knee. J Bone Joint Surg Am 2008;90(Suppl. 4):195—201.

[21] Banks SA, Hodge WA. Accurate measurement of three-dimensional knee replacement kinematics using single-plane fluoroscopy. IEEE Trans Biomed Eng 1996;43(6):638—49.

[22] Zuffi S, Leardini A, Catani F, Fantozzi S, Cappello A. A model-based method for the reconstruction of total knee replacement kinematics. IEEE Trans Med Imaging 1999;18:981—91.

[23] Mahfouz MR, Hoff WA, Komistek RD, Dennis DA. A robust method for registration of three-dimensional knee implant

models to two-dimensional fluoroscopy images. IEEE Trans Med Imaging 2003;22(12):1561—74.

[24] Kaptein BL, Valstar ER, Stoel BC, Rozing PM, Reiber JH. A new model-based RSA method validated using CAD models and models from reversed engineering. J Biomech 2003;36:873—82.

[25] Fukuoka Y, Hoshino A, Ishida A. A simple radiographic measurement method for polyethylene wear in total knee arthroplasty. IEEE Trans Rehabil Eng 1999;7:228—33.

[26] Van der Zwet PM, Meyer DJ, Reiber JH. Automated and accurate assessment of the distribution, magnitude, and direction of pincushion distortion in angiographic images. Invest Radiol 1995;30:204—13.

[27] Gronenschild E. Correction for geometric image distortion in the X-ray imaging chain: local technique versus global technique. Med Phys 1999;26(12):2602—16.